The Astrophysical Journal, 827:63 (5pp), 2016 August 10 doi:10.3847/0004-637X/827/1/63

ICE GRAIN COLLISIONS IN COMPARISON: CO_2, H_2O, AND THEIR MIXTURES

Grzegorz Musiolik, Jens Teiser, Tim Jankowski, and Gerhard Wurm
Fakultät für Physik, Universität Duisburg-Essen, Lotharstr. 1, D-47048 Duisburg, Germany
Received 2016 February 13; revised 2016 May 4; accepted 2016 June 7; published 2016 August 8

ABSTRACT

Collisions of ice particles play an important role in the formation of planetesimals and comets. In recent work, we showed that CO_2 ice behaves like silicates in collisions. The resulting assumption was that it should therefore stick less efficiently than H_2O ice. Within this paper, a quantification of the latter is presented. We used the same experimental setup to study collisions of pure CO_2 ice, pure water ice, and 50% mixtures by mass between CO_2 and water at 80 K, 1 mbar, and an average particle size of ∼90 μm. The results show a strong increase of the threshold velocity between sticking and bouncing with increasing water content. This supports the idea that water ice is favorable for early growth phases of planets in a zone within the H_2O and the CO_2 iceline.

Key words: planets and satellites: formation – protoplanetary disks

1. INTRODUCTION

Ices are important constituents in the collisional formation of comets and planetesimals in protoplanetary disks. As various species of ice appear in different distances to the central star due to their individual sublimation pressures, there are various icelines within the disk. Planet formation in general, but especially collisional outcomes, are tied to these icelines and the physics of the prevailing kind of ice. (Aumatell & Wurm 2011, 2014; Ali-Dib et al. 2014; Blum et al. 2014; Deckers & Teiser 2016; Musiolik et al. 2016).

In earlier experiments, we showed that it is necessary to distinguish the different ices while studying their growth potential (Musiolik et al. 2016). We suggested that collisional growth should be most efficient between the water and the CO_2 iceline or between 2.0 and 9.3 AU according to the minimum mass solar nebula model. Beyond 9.3 AU, non-polar CO_2 dominates. Collision experiments showed that CO_2 collisions are comparable to silicate collisions. An increased sticking of water ice was proposed but not verified in experiments.

H_2O is often considered as a driving mechanism for planetesimal growth due to a high sticking efficiency compared to other materials (Gundlach et al. 2011). While this is plausible as water does have a high electrical dipole moment and as individual experiments with water ice point to this (Gundlach & Blum 2015), a direct experimental comparison with other ices under similar conditions is missing. Therefore, we compare collisions of pure CO_2, pure H_2O, and 1:1 mixtures by mass here.

2. THE EXPERIMENT

2.1. Experimental Setup

The experimental setup is equal to the former experiment from Musiolik et al. (2016). Details can be found there. In short, the experiment consists of a vacuum chamber flooded with different gas samples. In the former experiment we used CO_2 gas. In this work, we additionally take a mixture between CO_2 and H_2O gases and H_2O vapor. A scheme of the experimental setup is shown in Figure 1.

The chamber is cooled by liquid nitrogen to a temperature of 80 K in the collision section. Within several minutes a 2 mm thick ice layer is deposited on the walls of the chamber. The chamber is sealed and evacuated to an ambient pressure of ∼1 mbar. By means of a gearwheel driven by an electrical motor, ice grains are beveled off from the cryostate. This produces ∼90 μm ice particles. The chemical composition of the produced aggregates depends on the gas (mixture) which was used to float the chamber. The particles collide with an ice layer of the same composition which is deposited on a copper plate connected to the cryostate. Collision velocities reach up to 1 m s^{-1} in this work. Collisions are imaged with a camera at 1250 frames per second with a spatial resolution of 10 μm.

2.2. Sample Preparation and Size Measurement

The colliding ice particles are generated by scraping them off from the cooled cryostate. The structure and the chemical composition of these aggregates depend on the initial atmosphere within the vacuum chamber.

For pure CO_2 aggregates the chamber is just continuously flooded by a stream of CO_2 gas. The CO_2 sublimation point is at about 195 K (Mazzoldi et al. 2008). Therefore, we argue that the molecules only freeze out once they hit a cold wall but do not already form ice grains within the gas phase. The scraping then removes material from a solid ice surface. According to our earlier analysis of fragmenting collisions, the CO_2 particles are small aggregates.

For the H_2O–CO_2 aggregates we use the same procedure with a mixture of CO_2 gas and H_2O vapor. The mass ratio between CO_2 and H_2O is 1:1. This value was determined after the experiment by weighing the mass loss of the ice mixture outside of the chamber, which is caused by the rapid evaporation of CO_2. Unlike the CO_2 vapor, the water supply already consists of ∼μm water droplets besides vapor. The structure of the ice surface will be slightly different then. We currently cannot analyze this in detail, but would argue on the state of the ice surface as follows.

Some of the water droplets will diffuse toward the walls and stick there as water ice grains. However, gas molecules will reach the surface by diffusion preferentially (due to their smaller mass compared to the droplets) and stick there as in the pure CO_2 case. This leads to an intimate mixture of CO_2 and water ice molecules with a certain amount of pure water ice grains embedded which can be regarded as homogeneous material. Our collision results are in favor of this view. As seen below, we see a clear threshold velocity between bouncing and sticking for particles from the mixed sample. This threshold is

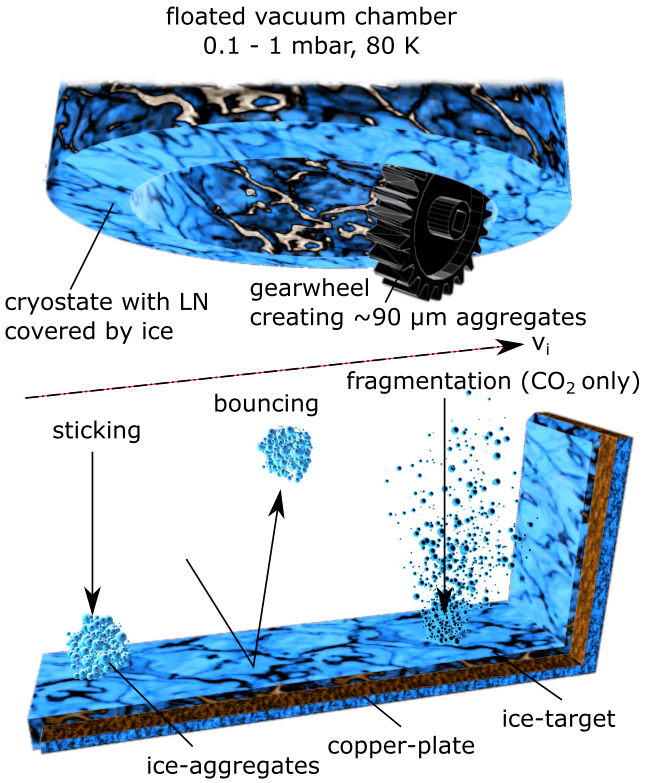

Figure 1. Experimental setup: a vacuum chamber is flooded with a gas (mixture) which is deposited on a cryostate cooled with liquid nitrogen. Then the chamber is evacuated to an ambient pressure of 0.1–1 mbar and particles are beveled off by using a rotating gearwheel. The particles collide with an ice layer on a copper plate connected to the cryostate. Depending on the impact velocity, sticking or bouncing can be observed. In an earlier work, we also observed fragmentation for CO_2 (Musiolik et al. 2016).

distinguished from the pure CO_2 threshold by an order of magnitude. If the particles which are beveled off were inhomogeneous and consist of large fractions of pure water or pure CO_2 ice or otherwise locally distinguished compositions at their surface, then an individual collision should depend on the material during contact which should, e.g., be water or CO_2 in a given collision. In any case, we should not see a clear threshold in collision experiments. The same argument holds if there is a significant amount of ice grains embedded but if scraping preferentially breaks the mixed matrix in between which is supposedly less stable. Also then, only one sort of mixed surface would interact with the same material. In this case, the mixing ratio might not be the mixing ratio of the matrix material measured (1:1) though, but might be shifted toward the CO_2 fraction. As the CO_2 fraction is high, in this case the mix will join together any pure water ice spheres efficiently, though. They might be porous, but the aggregates cannot restructure at the given impact energies and can be considered as individual grains for low velocities.

For the H_2O sample, we flooded the chamber only with water vapor and droplets. The same arguments hold that there should be a mixture of water ice droplets embedded in a water ice matrix. It is likely, though, that the water ice matrix is very thin and weak. In this case, it might not be appropriate to treat the aggregate particles as single grains, as small impact velocities might be sufficient to restructure the aggregate. Some elasticity in larger aggregates is clearly visible in the high-speed observations for the case of pure water ice. This changes

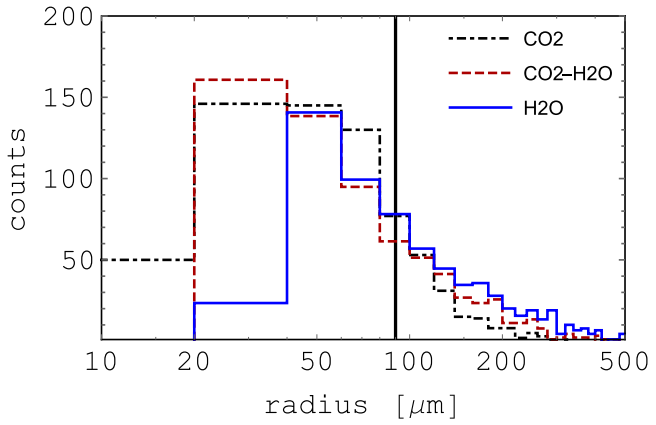

Figure 2. Size distribution for the different species of ice particles considered for this study. The distribution for the CO_2 aggregates is taken from Musiolik et al. (2016). The black line marks the average size of 90 μm. A bin size of 20 μm is chosen with respect to the spatial resolution of the camera.

the outcome of collisions (e.g., Dominik & Tielens 1997). It will depend on the specific configuration now and the amount of energy that is dissipated by restructuring if an aggregate sticks or bounces. We should not expect a clear threshold velocity.

We consider the pure CO_2 particles and mixed particles as solid spheres even if they would be aggregates. All particles are initially modeled as spheres of a size with the same cross sections as the observed grains. We determined the cross section by optical imaging. This way we get size distributions of the particles which can be found in Figure 2. These distributions are comparable; they all peak around ~50 μm and have a medium size of ~90 μm. The bin size of 20 μm is chosen due to the spatial resolution of the optical system of 10 μm. There is an indication in the size distribution of a cutoff at 20 μm. In any case, Krijt & Kama (2014) showed that there is a smallest fragment in a dissipative process so it is not likely that all particles will be covered by a layer of small unseen grains. Smaller particles may be present but should not affect the observed collisional outcomes.

The analyzed grain sizes are a narrow but representative illustration of dust found in protoplanetary disks. Here, the sizes reach from sub-μm, which is a typical size for dust in the ISM (Draine 2003; Williams & Cieza 2011), to the centimeter regime at which the bouncing barrier sets in (Zsom et al. 2010). The size distribution typically follows a power law (Draine 2006).

Since the distributions of all analyzed particles (Figure 2) are comparable, we can directly compare the collisional behavior for one mean size of the different species of ice grains depending on the collision velocity, though keeping in mind that aggregation might affect the result.

3. RESULTS AND DISCUSSION

Collisional outcomes at low speed can be categorized in two types: (1) sticking between the grain and the target at low velocities; (2) bouncing from the target at higher impact velocities (Weidenschilling & Cuzzi 1993, pp. 1031–1060; Blum & Wurm 2000; Ormel et al. 2007; Heißelmann et al. 2010; Zsom et al. 2010). The threshold between sticking and bouncing is not only important for understanding whether collisional growth of aggregates in protoplanetary disks is

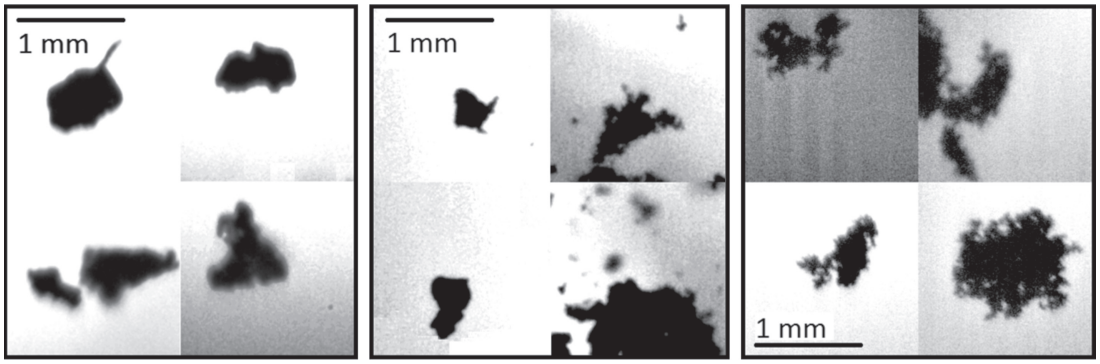

Figure 3. Structure of the largest aggregates from the data set for the various compositions. For each ice species, four aggregates are shown to illustrate the internal structures. The morphology of the water ice shows a high porosity in contrast to more compact morphologies otherwise.

possible, but also allows us to determine fundamental parameters like the surface energy of the particles (Dominik & Tielens 1997). In general, there are more effects for higher impact velocities like the fragmentation of or mass transfer to the aggregates (Blum & Wurm 2008; Deckers & Teiser 2016) which we do not consider in this work.

In Figure 3 we show samples of the largest aggregates for each data set of different ices (not analyzed collisionwise). For the largest aggregates, the surface structure and porosity can be determined easiest. Observation of these particles suggest a more irregular surface structure and higher porosity for water ice. A quantitative analysis of the surface and the porosity is not possible so far. As described above, due to the variation in the microstructure between the CO_2 aggregates and the CO_2–H_2O-/H_2O-aggregates, a comparison of their collisional behavior is given only roughly.

The porous structure of the water ice aggregates suggests that restructuring might be important as indicated above. The mixed ice samples qualitatively look compact enough that they should only show hit-and-stick or just bouncing slightly above the threshold for sticking.

More quantitatively, the collisional behavior can be described by the coefficient of restitution (COR), which we define as the ratio of the absolute value of the particle velocity after v_o and before v_i the collision

$$\epsilon = \frac{v_o}{v_i}. \tag{1}$$

There are many theoretical models describing the COR for elastic, plastic, and viscous spheres (Andrews 1930; Thornton & Ning 1998; Tomas 2006; p. 183). Other approaches try to describe the COR by heuristic functions, like Higa et al. (1996, 1998) did for water ice spheres. For the COR resulting from the observed collisions, we use our model deduced in the earlier work on pure CO_2 collisions (Musiolik et al. 2016)

$$\epsilon(v_i) = A \cdot e^{\left(a_1\left(\ln\left(\frac{v_i - v_{stick}}{v_c}\right)\right)^2\right)}\Theta(v_i - v_{stick}) \tag{,2}$$

with the critical velocity v_c, the sticking velocity v_{stick}, and material depended parameters a_1 and A. Here, the sticking velocity v_{stick} describes the transition between the sticking and the bouncing regime, where $\epsilon(v \leqslant v_{stick}) = 0$ and $\epsilon(v > v_{stick}) > 0$. The critical velocity v_c describes the maximum for the COR, where the bouncing is most elastic. The COR from Equation (2) models three different effects; sticking with $\epsilon(v \to 0) \to 0$, elastic bouncing with $\max(\epsilon(v)) = \epsilon(v_c)$, and plastic deformation with $\epsilon(v \to \infty) \to 0$. This function gives the most appropriate fit for the COR for CO_2 particles. It also fits the COR for the H_2O/CO_2 mixture well like shown in Figure 4. The fit parameters for both fits are summarized in Table 1.

The gravitational force is acting on the aggregates during collisons. This effect distorts the analysis of the data, because low COR collisions might be classified as sticking events. Nonetheless, in Musiolik et al. (2016) we show that this effect becomes significant only for collisions with impact velocities below $0.05\,\mathrm{m\,s^{-1}}$. This is also the reason for deducing the sticking velocity for CO_2 aggregates by a model fit in the previous work.

Collisions of CO_2–H_2O particles are more inelastic than collisions of CO_2, since the COR in Figure 4 has smaller values for the mixture. Moreover, the sticking velocity is an order of magnitude larger. From the sticking velocity, we can calculate the surface energy for CO_2–H_2O particles from (Dominik & Tielens 1997)

$$v_{stick} = \frac{1.07}{\rho^{1/2}E_{py}^{1/3}} \cdot \frac{1}{R^{5/6}} \cdot \gamma^{5/6}, \tag{3}$$

with the surface energy γ, the reduced radius R, the particle mass density ρ, and an elastic constant E_{py}, where $E_{py} = E_y/(2(1-\nu_p^2))$. In this definition, E_y is the Young's modulus and ν_p is the Poisson's ratio.

Taking a mean Young's modulus between water ice and CO_2 ice of $E_y = 1/2(13 + 9)$ GPa, a mean density of $\rho = 1/2\,(1000 + 1560)\,\mathrm{kg\,m^{-3}}$, and a mean poisson ratio of $\nu_p = 1/2\,(0.3 + 0.28)$ (Yamashita & Kato 1997; Nimmo 2004; Musiolik et al. 2016), we get a surface energy for particles with a mean radius of $r_p = 90 \pm 20\,\mu\mathrm{m}$ of

$$\gamma_{mix} = 2.77^{+0.9}_{-0.8}\,\mathrm{J\,m^{-2}}. \tag{4}$$

We determined the surface energy for pure CO_2 ice in our earlier work to $\gamma_{CO2} = 0.17\,\mathrm{J\,m^{-2}}$ (Musiolik et al. 2016). Compared to this the surface energy of mixed particles is an order of magnitude higher.

For the H_2O aggregates, we do not see a sharp transition from the sticking regime to the bouncing regime, which might be due to the preparation and restructuring of the aggregates in

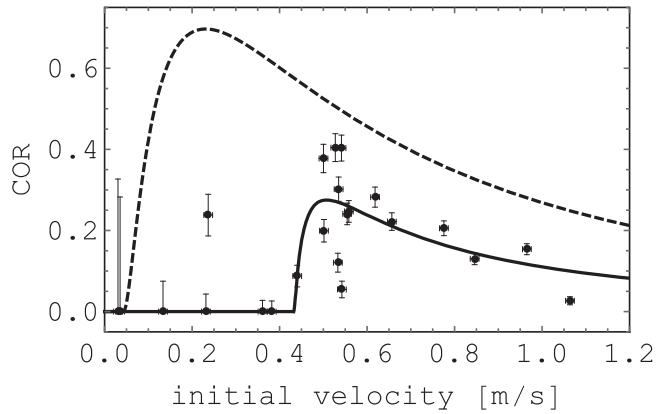

Figure 4. Coefficient of restitution (COR) for the mixture particles with a H_2O–CO_2 mass ratio of 1:1. The dashed line describes the COR for pure CO_2 particles from Musiolik et al. (2016). The solid line represents the fit function from Equation (2). The uncertainties result from uncertainties in the impact velocity and the aggregate size.

Table 1
Fit Parameters for the COR

	CO_2	CO_2–H_2O
A	0.67 ± 0.04	0.27 ± 0.05
a_1	-0.36 ± 0.04	-0.22 ± 0.4
v_c [m s^{-1}]	0.189 ± 0.025	0.075 ± 0.12
v_{stick} [m s^{-1}]	0.04 ± 0.02	0.43 ± 0.03

Note. The values for CO_2 particles are taken from Musiolik et al. (2016).

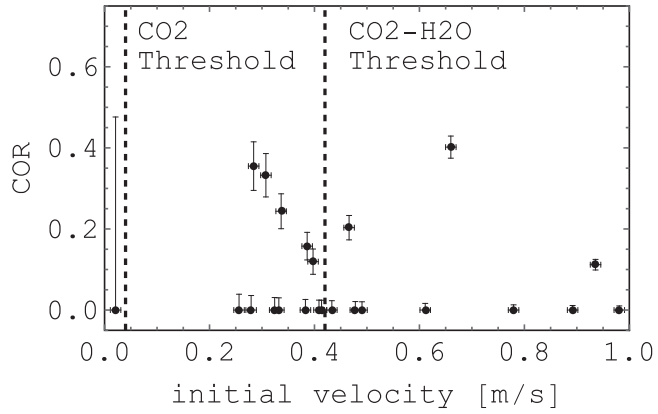

Figure 5. Coefficient of restitution (COR) for water ice particles. The dashed lines describe the threshold for CO_2 and CO_2–H_2O data.

collisions. Figure 5 shows the measured data for the COR. We can determine a sticking probability P though, defined as the ratio between all sticking events in collisions N_s and all analyzed collison events N for a certain velocity range

$$P = \frac{N_s}{N}. \quad (5)$$

For impact velocities between 0 and 0.5 m s^{-1}, the sticking probability is $P = 0.65$ and for impact velocities between 0.5 and 1 m s^{-1} $P = 0.67$.

For comparability of pure water ice, one can use Equation (3) to get a rough estimate of the dependency between the H_2O fraction p_W in the particles and the sticking velocity $v_{stick}(p_W)$ for the range $p_W \in [0, 1]$. Assuming a simple linear approximation of $\gamma \propto p_W + \xi_1$ with the constants ξ_1, ξ_2 we obtain

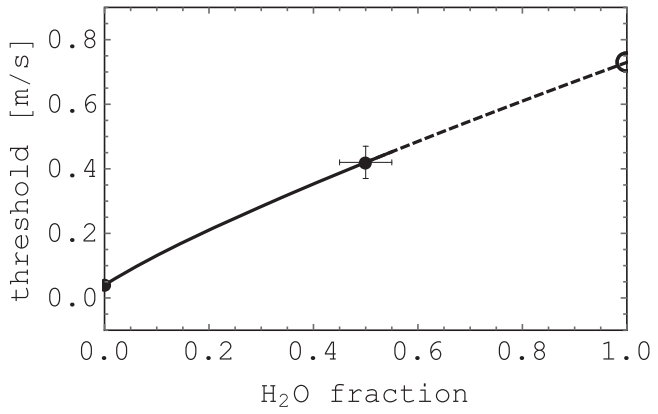

Figure 6. Threshold velocities between the sticking and the bouncing regime depending on the H_2O fraction of the ice. The black dots show measured values and the circle an estimation from Equation (6). The black line shows the fit function which changes over to the extrapolation.

$$v_{stick}(p_W) = \xi_2 (p_W + \xi_1)^{5/6}. \quad (6)$$

Using Equation (6), we can fit the sticking velocities determined for $p_W = 0$ and $p_W = 0.5$ and extrapolate this function for an H_2O fraction of 1. For the constants we get $\xi_1 = 0.031$ and $\xi_2 = 0.711$ m s^{-1}. This procedure leads to a value of $v_{stick}(1) \approx 0.73$ m s^{-1} (Figure 6). Within the range studied we do see sticking and bouncing of pure water ice at this velocity. The measured water data is therefore at least not in contradiction to this extrapolation.

In their recent, work Gundlach & Blum (2015) give a sticking threshold for 1.5 μm-sized water ice of 9.6 m s^{-1}. If we scale this value with the dependency from Equation (3), $v_{stick} \propto R^{-5/6}$, we get a sticking velocity of 0.31 m s^{-1} for 90 μm pure water ice grains. Within the range of unknowns (porosity, regular–irregular grain relation) our data are also consistent with this.

4. CAVEATS

Figure 6 clearly shows that threshold velocities for sticking of H_2O/CO_2 mixtures vary between the less sticky end member CO_2 and the much stickier other end of pure H_2O ice. The analytical dependence between γ and p_W chosen—or in general the sticking velocity dependence on p_W—could be more complex, however. In general, the JKR theory can give us only an approximation here because it does not describe non-spherical aggregate shapes and complicated contacts including dipole moments or hydrogen bonds. A more detailed analysis based on thorough variation of the mass ratios (p_W) would be needed to quantify this further. However, as outlined above, the preparation does not warrant homogeneous mixtures yet but grains might, e.g., be core-mantle particles with embedded water ice grains. In this case, the total mass ratios determined by sublimation of the CO_2 afterwards could be different from mass ratios of the surfaces which are actually in contact during a collision. Hence, such a study would require a spatially resolved analysis of the composition of the grains on the nanometer scale. This seems feasible with current microscopic techniques, but due to the volatile nature of the ices, this is not straightforward and is beyond the scope of this paper.

We used the sticking velocity measured and modeled as given and deduced the surface energy based on Equation (3). This might lead to a mismatch with given literature data. Values for the surface energy of pure H_2O ice are, e.g., $0.37\,J\,m^{-2}$ from Hirashita & Li (2013) or $0.19\,J\,m^{-2}$ from Gundlach et al. (2011) and Blum et al. (2014). Our value of the mixed sample should be below the water value and the determined value of $2.8\,J\,m^{-2}$ looks to be too large then (by an order of magnitude). Our deduced values for pure CO_2 is also overestimating existing values by a factor of a few (Musiolik et al. 2016). Experimental work from Blum & Wurm (2000) and Poppe et al. (2000) suggested that the model by Dominik & Tielens (1997) might give values for v_{stick} that are an order of magnitude too low. If this is a theoretical (model)/experimental mismatch, our deduced values from Equation (3) could be overestimated by an order of magnitude, though they would be self-consistent among themselves. Another uncertainty in the calculation of the surface energy is the structure of the particles. For once they are irregular and not spheres and likely can be small aggregates. With the optical observation used, we cannot resolve the particles further and do not precisely know the total mass. We used bulk densities instead. In total, the value in Equation (4) should rather be treated as an estimation than an exact result at the moment. This does not devalue the qualitative dependence of the sticking velocity with water content, however.

5. CONCLUSION

In this work, we measured the threshold velocity between sticking and bouncing for collisions of ice grains with a solid wall of the same material. We studied three compositions: pure dry ice, pure water ice, and a 1 to 1 mixture. As we used the same setup, the results are immediately comparable. In all three cases, the average particle size analyzed was $\sim 90 \pm 20\,\mu m$. Collision velocities were up to $1\,m\,s^{-1}$. Our goal was to show explicitly how by comparison the sticking properties of these ices differ in collisions.

While CO_2 particles of the given size only stick at velocities below $0.04\,m\,s^{-1}$, mixtures of 1:1 mass ratio have a sticking threshold at $0.43\,m\,s^{-1}$. For pure H_2O ice, we could not find a steep threshold velocity but only probabilities on the order of 60%–70% for sticking up to $1\,m\,s^{-1}$, which is likely caused by a fragile aggregate structure. From the sticking velocity for the particles consisting of the mixture of H_2O/CO_2 ice, we calculate the surface energy to $\gamma = 2.77^{+0.9}_{-0.8}\,J\,m^{-2}$. Compared to pure CO_2 ice, this is an order of magnitude higher, though the quantitative derivation of this values should be considered with care.

In our earlier paper, we showed that CO_2 behaves mostly like silicates (Musiolik et al. 2016). Here, we show that adding water makes particles much stickier. This supports the idea that there is an inner, silicate-dominated region and and outer, CO_2-dominated region in protoplanetary disks where collisional growth might be less efficient than in the region in between the respective icelines where water ice dominates.

This work is supported by the DFG under the grant number WU321/12-1 and TE890/1-1.

REFERENCES

Ali-Dib, M., Mousis, O., Petit, J.-M., & Lunine, J. I. 2014, ApJ, 793, 9
Andrews, J. 1930, The London, Edinburgh, and Dublin Philosophical Magazine and Journal of Science, 9, 593
Antonyuk, S., Heinrich, S., Tomas, J., et al. 2010, Granular Matter, 12, 15
Aumatell, G., & Wurm, G. 2011, MNRAS, 418, L1
Aumatell, G., & Wurm, G. 2014, MNRAS, 437, 690
Blum, J., Gundlach, B., Mühle, S., & Trigo-Rodriguez, J. M. 2014, Icar, 235, 156
Blum, J., & Wurm, G. 2000, Icar, 143, 138
Blum, J., & Wurm, G. 2008, ARA&A, 46, 21
Deckers, J., & Teiser, J. 2016, MNRAS, 456, 4328
Dominik, C., & Tielens, A. G. G. M. 1997, ApJ, 480, 647
Draine, B. T. 2003, ApJ, 598, 1026
Draine, B. T. 2006, ApJ, 636, 1114
Gundlach, B., & Blum, J. 2015, ApJ, 798, 34
Gundlach, B., Kilias, S., Beitz, E., & Blum, J. 2011, Icar, 214, 717
Heißelmann, D., Blum, J., Fraser, H. J., & Wolling, K. 2010, Icar, 206, 424
Higa, M., Arakawa, M., & Maeno, N. 1996, P&SS, 44, 917
Higa, M., Arakawa, M., & Maeno, N. 1998, Icar, 133, 310
Hirashita, H., & Li, Z.-Y. 2013, MNRAS, 434, L70
Krijt, S., & Kama, M. 2014, A&A, 566, L2
Mazzoldi, A., Hill, T., & Colls, J. J. 2008, International Journal of Greenhouse Gas Control, 2, 210
Musiolik, G., Teiser, J., Jankowski, T., & Wurm, G. 2016, ApJ, 818, 16
Nimmo, F. 2004, in Workshop on Europa's Icy Shell: Past, Present, and Future, ed. P. Schenk, F. Nimmo, & L. Prockter, 7005
Ormel, C. W., Spaans, M., & Tielens, A. G. G. M. 2007, A&A, 461, 215
Poppe, T., Blum, J., & Henning, T. 2000, ApJ, 533, 454
Thornton, C., & Ning, Z. 1998, Powder Technology, 99, 154
Tomas, J. 2006, Particles on Surfaces, vol. 8
Weidenschilling, S. J., & Cuzzi, J. N. 1993, in Protostars and Planets III, ed. E. H. Levy & J. I. Lunine, (Tucson, AZ: Univ. of Arizona Press), 1031
Williams, J. P., & Cieza, L. A. 2011, ARA&A, 49, 67
Yamashita, Y., & Kato, M. 1997, GeoRL, 24, 1327
Zsom, A., Ormel, C. W., Güttler, C., Blum, J., & Dullemond, C. P. 2010, A&A, 513, A57